MAPPING FORESTS:
A multitemporal analysis

EDUARDA MARTINIANO DE OLIVEIRA SILVEIRA

2007

EDUARDA MARTINIANO DE OLIVEIRA SILVEIRA

MAPPING FORESTS:
A multitemporal analysis

Dissertação apresentada à Universidade Federal de Lavras como parte das exigências do curso de mestrado em Engenharia Florestal, área de concentração em Manejo Ambiental, para obtenção do título de "Mestre".

Orientador:

Prof. Luis Marcelo Tavares de Carvalho

Co-orientador:
Prof. Fausto Weimar Acerbi Jr.

LAVRAS
MINAS GERAIS – BRASIL

Ficha Catalográfica Preparada pela Divisão de Processos Técnicos da Biblioteca Central da UFLA

Silveira, Eduarda Martiniano de Oliveira.
Mapping forests: a multitemporal analysis / Eduarda Martiniano de Oliveira Silveira. -- Lavras : UFLA, 2007.
75 p. : il.

Dissertação (Mestrado) – Universidade Federal de Lavras, 2008.
Orientador: Luis Marcelo Tavares de Carvalho.
Co-orientador: Fausto Weimar Acerbi Jr.
Bibliografia.

1. Classificação. 2. Séries temporais. 3. Extração de feições. 4. Fusão de imagem. I. Universidade Federal de Lavras. II. Título.

CDD -621.3678

EDUARDA MARTINIANO DE OLIVEIRA SILVEIRA

MAPPING FORESTS: A multitemporal analysis

Dissertação apresentada à Universidade Federal de Lavras como parte das exigências do curso de mestrado em Engenharia Florestal, área de concentração em Manejo Ambiental, para obtenção do título de "Mestre".

APROVADA em 09 de agosto de 2007.

Prof. Dr. José Márcio de Mello – UFLA.

Prof. Dr. Yosio Edemir Shimabukuru – INPE.

Prof. Dr. Laerte Guimarães Ferreira - UFG

Prof. Dr. Luis Marcelo Tavares de Carvalho.
UFLA
(Orientador)

LAVRAS
MINAS GERAIS – BRASIL

Humberto M. R. da Silveira
Maria Cláudia M. O. Silveira
Maurício M. O. Silveira
Aos eternos amigos

Dedicate

ACKNOWLEDGEMENT

Adauta Copertino de Oliveira
Adalberto Caldas Oliveira
Alan de Brito (Cabritão)
Allan Arantes Pereira (Titio)
Ançano Loschi Neto
Antônio Cláudio David
Antônio Couto Souza Júnior
Antonio Donizete de Oliveira
Antônio Marciano da Silva
Carlos Augusto Z. Tonelli (Guto)
Carlos Henrique G. (Carlotinha)
CAPES
Clair Rogério da Cruz
Costelinha
Daniela Duarte Ventura Melo
Eduane José de Pádua
Elizabeth Costa Rezende Abreu
Fabio Camolesi (Zigoto)
Fausto Weimar Acerbi Júnior
Francisco Bernardes (Chicão)
Gláucia
Gleyce Campos Dutra (Cleide)
Henriqueta Veloso Ferreira
Bernardi
José Marcio de Mello
José Roberto Scolforo
Luciano T. de Oliveira (Bodinho)
Luis Antônio C. Borges (Totonho)
Luis Carvalho (Passarinho)
Maira Dzedzej
Marcela Duarte (Capetão)
Marco Aurélio Leite (Espeto)
Mariana Oppido (Xuxu)
Marquinho (Guelas)
Montana
Poliana Costa Lemos
Postinho
Rafael Costa Mariano (Rafinha)
Raphael Medina Gomes de Andrade
Ricardo da S. Carvalho (Clavicola)
Samuel Campos Sales
Suzana Rodriguez Vieira
Núcleo de Manejo Florestal
(LEMAF)

SUMMARY

ABSTRACT…… i
RESUMO……. ii
CHAPTER 01: General introduction……... 1
CHAPTER 02: The assessment of vegetation seasonal dynamics using multitemporal NDVI and EVI images derived from MODIS 4
Abstract……..…. 5
Resumo……. 6
1 Introduction…….. 7
2 Material and Methods…….…….... 10
3 Results and Discussion…… 15
4 Conclusions…….. 21
5 Bibliographical References 22
CHAPTER 03: Multiscale feature extraction of MODIS multitemporal vegetation index using wavelets……... 25
Abstract…… 26
1 Introduction…….. 27
2 Methods……. 29
2.1 Study area and MODIS data……... 29
2.2 Feature extraction……. 32
2.3 Classification procedure……... 38
3 Results and discussion……. 40
4 Conclusions…….. 44
5 Bibliographical references…….. 45
CHAPTER 04: Multisensor image fusion and multiscale feature extraction on classification accuracy……. 47
Abstract…… 48
1 Introduction…….. 49
2 Methods……. 52
2.1 Study area…….. 52
2.2 Data…… 53
2.3 Fusion procedure…….. 55
2.4 Quality assessment…… 56
2.5 Feature extraction……. 57
2.6 Classification procedure……... 60
3 Results and discussion……. 62
3.1 Quality assessment…… 62
3.2 Classification procedure……... 65
4 Conclusions…….. 68
5 References……. 69
CHAPTER 05: General conclusions……. 72

ABSTRACT

SILVEIRA, Eduarda Martiniano de Oliveira. **Mappinf forests: A mutiltemporal analysis.** 2007. 75 p. Dissertação (Mestrado em Manejo Ambiental) – Universidade Federal de Lavras, Lavras, MG.[1]

The North of Minas Gerais, Brazil, characterized by extensive cerrado areas, semideciduous and deciduous forest was chosen to validate the hypothesis that long time series combined with feature extraction algorithm and image fusion can be used to improve classification accuracy. Thus, this study was organized in five chapters. The first is a General Introduction. Chapter 02 evaluated the seasonal dynamics of this vegetation classes by analyzing time series of NDVI and EVI derived from MODIS sensor. On Chapter 03 the potential of the discrete wavelet transform in order to extract features to improve classification accuracy was tested. The objective of Chapter 04 was to assess the potential of using fused images between MODIS and TM images as well as feature extraction algorithm combined with image fusion to produce accurate maps. Chapter 05 is as General Conclusion. As a conclusion (1) the vegetation indices (NDVI and EVI) temporal profiles were efficient to depict the seasonal dynamics of vegetation and the best index for mapping was the NDVI; (2) The Wavelet decomposition improved land cover classification accuracy when the algorithm used in the transformation and the levels were properly chosen; (3)The data fusion and feature extraction method performed well in terms of overall accuracies as compared to results obtained by the original time series of NDVI.

Key-words: Classification; time series; feature extracion; image fusion.

Comitê orientador: Luis Marcelo Tavares de Carvalho – UFLA (Orientador); Fausto Weimar Acerbi Junior – UFLA (Co-orientador); José Márcio de Mello – UFLA; Yosio Edemir Shimabukuro – INPE; Laerte Ferreira Guimarães – UFG.

RESUMO

SILVEIRA, Eduarda Martiniano de Oliveira. **Mappinf forests: A mutiltemporal analysis.** 2007. 75 p. Dissertação (Mestrado em Manejo Ambiental) – Universidade Federal de Lavras, Lavras, MG.[2]

O Norte do estado de Minas Gerais, caracterizado por grandes áreas de cerrado, floresta estacional semidecidual e decidual foi escolhido para validar a hipótese de que séries temporais juntamente com algoritmos de extração de feições e fusão de imagens podem ser utilizados para aperfeiçoar a acurácia da classificação de imagens. Assim este estudo foi organizado em cinco capítulos. O capítulo 01 é uma introdução geral. O capítulo 02 avaliou a dinâmica sazonal da vegetação analisando as séries temporais dos índices de vegetação NDVI e EVI do sensor MODIS. No capítulo 03 o potencial da transformada em ondaletas discreta para extração de feições no aperfeiçoamento da classificação foi testado. O objetivo do capítulo 04 foi avaliar o potencial da fusão de imagens entre os sensores MODIS e TM, bem como algoritmos de extração de feições combinados com fusão de imagens com o intuito de aprimorar a classificação. O capítulo 05 é uma conclusão geral. Concluiu-se que (1) as assinaturas temporais dos índices de vegetação NDVI e EVI foram eficientes para detectar a dinâmica sazonal da vegetação e o melhor índice foi o NDVI; (2) a transformada em ondaletas aperfeiçoou a classificação da vegetação quando o algoritmo utilizado na transformação e os níveis de decomposição foram adotados corretamente; (3) a fusão de imagens e o método de extração de feições obtiveram bons resultados em termos de acurácia global quando comparados com resultados obtidos apartir das séries temporais de NDVI.

Palavras-chave: Classificação; série temporal; extração de feições; fusão de imagens.

[2] Comitê orientador: Luis Marcelo Tavares de Carvalho – UFLA (Orientador); Fausto Weimar Acerbi Junior – UFLA (Co-orientador); José Márcio de Mello – UFLA; Yosio Edemir Shimabukuro – INPE; Laerte Ferreira Guimarães – UFG.

CHAPTER 01

1 GENERAL INTRODUCTION

The mapping of land cover types with similar reflectance behavior is a problem when the spectral information is provided by a single remotely sensed image.

However, the spectral behavior of these land cover classes may be identified when they are analyzed along the annual cycle, including both the dry and the rainy seasons. Thus, long time series combined with feature extraction algorithms and image fusion can be used to improve the separation of spectrally similar objects and produce accurate maps.

To validate this hypothesis an area of the State of Minas Gerais, characterized by extensive cerrado areas, semideciduous and deciduous forest was chosen. The MODIS vegetations indices, covering the rainy and dry season of 2003, 2004 and 2005 were analyzed and classified in order to produce accurate maps of the study area.

This study was motivated by problems that start with these questions:

(1) Can MODIS vegetation indices depict vegetation dynamics?

(2) Can feature extractions algorithms improve classification accuracy?

(3) Can image fusion combined with feature extraction algorithm improve classification accuracy?

To answer these questions this study was organized in five chapters listed below:

CHAPTER 01. General Introduction.

CHAPTER 02. The assessment of vegetation seasonal dynamics using multitemporal NDVI and EVI images derived from MODIS.

On this Chapter we evaluated the seasonal dynamics of cerrado, deciduous and semideciduous forest in the north of Minas Gerais, Brazil, using time series of NDVI and EVI derived from MODIS. They were compared by analyzing temporal profiles and image classification results.

CHAPTER 03. Multiscale feature extraction of MODIS multitemporal vegetation index using wavelets.

On this Chapter the use of NDVI time series and the 1D version of the algorithm "à trous" with linear and cubic spline wavelets to improve classification accuracy was analyzed. After decomposition, the smoothed signatures were used as feature vectors in the classification as well as the original time series of NDVI.

CHAPTER 04. Multisensor image fusion and multiscale feature extraction on classification accuracy.

The objective of this chapter was to assess the potential of using fused images between MODIS and TM images as well as feature extraction algorithm combined with image fusion to produce accurate maps.

CHAPTER 05. General Conclusions.

CHAPTER 02

THE ASSESSMENT OF VEGETATION SEASONAL DYNAMICS USING MULTITEMPORAL NDVI AND EVI IMAGES DERIVED FROM MODIS

Eduarda Martiniano de Oliveira Silveira[1], Luis Marcelo Tavares de Carvalho[1], Fausto Weimar Acerbi-Júnior[1], José Marcio de Mello[1]

[1]Federal University of Lavras – UFLA - PO Box 3037 - 37200-000 - Lavras-MG, Brazil - dudalavras@hotmail.com

(Prepared according to CERNE)

Abstract: The objectives of this work were to characterize seasonal dynamics of cerrado, deciduous and semideciduous forests in the north of Minas Gerais, Brazil. Time series of NDVI (Normalized Difference Vegetation Index) and EVI (Enhanced Vegetation Index) derived from MODIS sensor, were compared by analyzing temporal profiles and image classification results. The results showed that: (1) there is an agreement between vegetation indices and the monthly precipitation pattern; (2) deciduous forest showed the lowest values and the highest variation; (3) cerrado and the semideciduous forest presented higher values and lower variation; (4) based on the classification accuracies the best vegetation index for mapping the vegetation classes in the study area was the NDVI, however both indices might be used to assess the vegetation seasonal dynamic; and (5) further research need to be carried out exploring the use of feature extractions algorithms to improve classification accuracy of cerrado, semideciduous and deciduos forests in Minas Gerais, Brazil.

Keywords: Remote sensing, time series, vegetation indices.

Resumo: *O objetivo deste trabalho foi caracterizar a dinâmica sazonal do cerrado, floresta estacional semidecidual e decidual no norte do estado de Minas Gerais, Brasil. Séries multitemporais dos índices de vegetação NDVI (índice de vegetação da diferença normalizada) e EVI (índice de vegetação melhorado) derivados do sensor MODIS, foram comparadas analisando o perfil temporal e os resultados de classificação das imagens. Os resultados mostraram que: (1) Os índices de vegetação estudados refletiram o padrão sazonal das fisionomias, diferenciando os períodos chuvosos e os períodos de seca; (2) a fisionomia floresta estacional decidual apresentou menores valores dos índices e maior variação; (3) as fisionomias cerrado e floresta estacional semidecidual apresentaram alto valores dos índices e baixa variação; (4) de acordo com os resultados das classificações o melhor índice para o mapeamento das fisionomias na área de estudo foi o NDVI, porém ambos podem ser usados para avaliar a dinâmica sazonal da vegetação; e (5) estudos precisam ser realizados explorando algoritmos de extração de feições para melhorar a acuracidade do mapeamento das fisionomias cerrado, floresta decídua e semidecidua na área de estudo.*

Palavras chave: *Sensoriamento remoto, série multitemporal, índices de vegetação.*

1 INTRODUCTION

Maps of the distribution and status of the Earth's vegetation and land cover are critical for parameterization of global climate and ecosystem process models as well as characterization of the distribution and status of major land surface types for environmental, ecological and natural resource applications at global and regional scales (Muchoney et al., 2000).

The seasonal behavior of vegetation is a fundamental component of successful image interpretation (Lillesand & Kiefer, 1987). For land cover assessment, the timing of image acquisition can be critical. Knowledge of crop calendars and phenology is often a crucial element in vegetation interpretation. Since the 1970s, researches have recognized the potential of multitemporal satellite observations to provide information about the phenological development of natural vegetation and crops (Reed et al., 1994) moreover the combination of vegetation indices with multitemporal imagery that captures phenology has produced successful vegetation classifications (Sader et al., 1990).

Because of the synoptic coverage and repeated temporal sampling that satellite observations afford, remotely sensed data possess significant potential for monitoring vegetation dynamics (Myneni et al., 1997). Satellite vegetation index (VI) data such as the Normalized Difference Vegetation Index (NDVI) are

correlated with green leaf area index (LAI), green biomass, and percent green vegetation cover (Asrar et al., 1989; Baret & Guyot, 1991).

The radiometric and geometric properties of the Moderate Resolution Imaging Spectroradiometer (MODIS) onboard NASA's Terra spacecraft, in combination with improved atmospheric correction and cloud screening, provide a substantially improved basis for studies of this nature (Zhang et al., 2002). The MODIS instrument has 36 spectral bands that range from 250 m to 1 km where seven spectral bands are specifically designed for land applications (Justice et al., 1997).

The MODIS VI products provide consistent, spatial and temporal comparisons of global vegetation conditions which are used to monitor the Earth's terrestrial photosynthetic vegetation activity in support of phenologic, change detection, and biophysical interpretations. Two VI algorithms were produced. One is the NDVI, which is referred to as the continuity index to the existing NOAA-AVHRR derived NDVI. The other is an enhanced vegetation index (EVI) with improved sensitivity into high biomass regions and improved vegetation monitoring through a de-coupling of the canopy background signal and a reduction in atmosphere influences. This two VIs complement each other in global vegetation studies and improve upon the extraction of canopy biophysical parameters (Huete et al., 1997).

Thus, this study was motivated by the following research questions: (1) Are MODIS vegetation indices (NDVI and EVI) able to depict the seasonal dynamics of cerrado, deciduous and semideciduous forest? (2) What is the best vegetation index (VI) to map different land cover types in the study area?

The general objectives of this study were: (1) To characterize the seasonal vegetation dynamics captured by NDVI and EVI; (2) To compare the performance of NDVI and EVI temporal profiles for image classification.

2 MATERIAL AND METHODS

The study area (Figure 1) is located in the state of Minas Gerais, Brazil and is delimited by the coordinates S 14º 47' 25'' - S 15º 53' 16" and W 43º 52' 52'' - W 45º 6'17''. The area is cover by three major land cover types: deciduous forest, semideciduous forest and cerrado (Brazilian savannas).

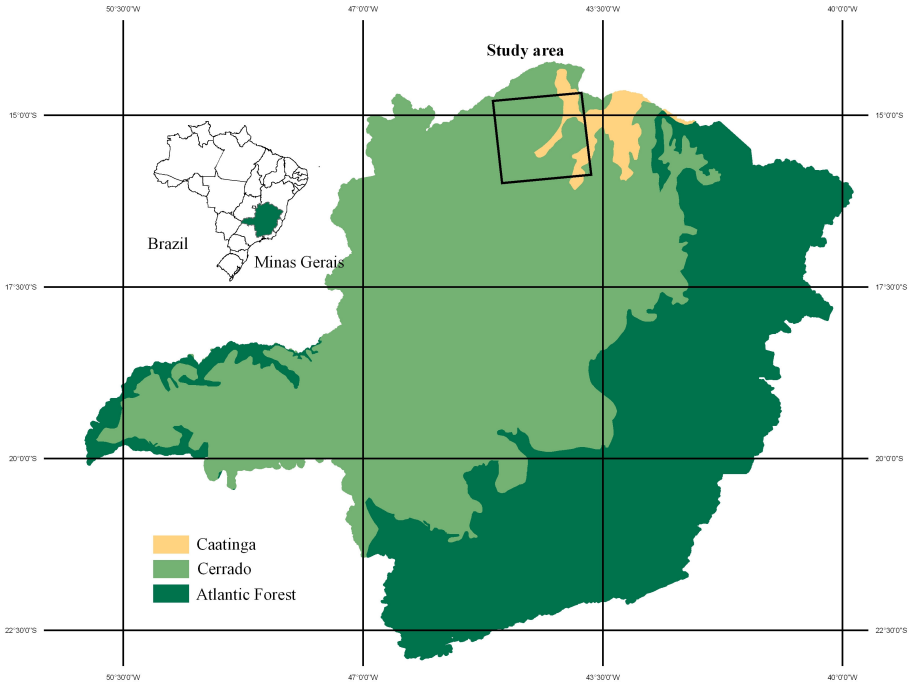

Figure 1 – Study area.

Figure 1 *– Área de estudo.*

Figure 2 shows the seasonal patterns in monthly precipitation for the year 2003, 2004 and 2005 as well as the historical data for the last 31 years.

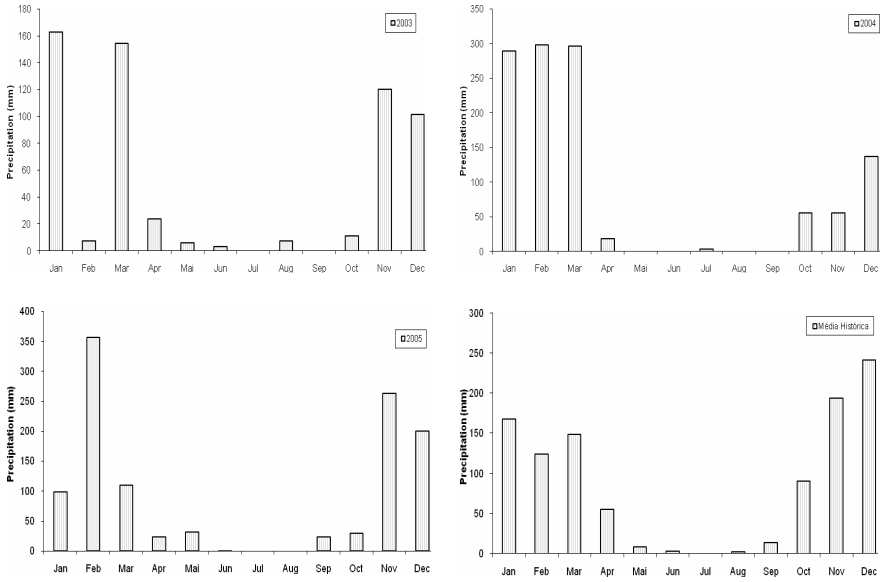

Figure 2 – Monthly precipitation pattern.

Figura 2 – *Precipitação média mensal.*

MODIS 16-day vegetation indices composite with 250 m of spatial resolution from TERRA satellite, were used to derive three years (2003, 2004 and 2005) NDVI and EVI temporal profiles. The images were resampled to Albers Conic Equal Area projection.

Along with the image data, there exists a map that associates a quality assurance number (QA) with each pixel of the image. The QA is a 16 bit coded integer. The various groups of this 16 bit long binary code describe different properties of the pixel. One can set thresholds or specific values for these different groups to check the 'quality' of the pixel and then label it either good or bad depending upon the application.

The quality assessment (QA) was carried out through MODIS metadata in order to ensure that the images were generated without errors or artifacts. Quality assessment bits from each data indicted data of good quality.

The NDVI is a normalized transform of the near infrared (NIR) to red reflectance ratio, ρ nir/ ρ red , designed to standardize VI values between –1 and +1 formulated as:

$$NDVI = \left[\frac{\rho nir - \rho red}{\rho nir + \rho red} \right] \qquad (1)$$

In spite of the intensive use of the NDVI and its variety of applications, several limitations of the index are known. Among these are the sensitivity for soil (especially dark and/ or wet) background (Huete et al., 1991), saturation of the index values in case of dense and multilayered canopy (Lillesaeter, 1982), and sensitivity for atmospheric influence (Holben, 1986) since aerosol increases the apparent reflectance in the red band by scattering sunlight directly to the sensor and decreases to a lesser degree the reflectance in the NIR by absorption of sunlight (Fraser & Kaufman, 1985).

Liu & Huete (1995) developed a feedback based approach to correct for the interactive canopy background and atmospheric influences, incorporating both background adjustment and atmospheric resistance concepts. This enhanced, soil and atmosphere resistant vegetation index (EVI) was simplified to:

$$EVI = 2.5\frac{(\rho_{nir} - \rho_{red})}{(L + \rho_{nir} + C_1\rho_{red} + C_2\rho_{blue})} \qquad (2)$$

Where ρ is 'apparent' (top-of-the-atmosphere) or 'surface' directional reflectances, L is a canopy background adjustment term, and C_1 and C_2 weigh the use of the blue channel in aerosol correction of the red channel (Huete et al., 1994). The blue band is sensitive to atmospheric conditions and is often used for atmospheric correction. EVI directly adjusts the reflectance in the red bands as a function of the reflectance in the blue band (Huete et al., 2002).

A set of 200 homogeneous pixels distributed over the area were randomly selected from each land cover type in order to generate the NDVI and EVI temporal profiles and characterize seasonal dynamics of the vegetation. The selection was based on field campaigns, as well as on a vegetation map produced at the Federal University of Lavras - UFLA (Scolforo & Carvalho, 2006).

Additionally, the NDVI and EVI multitemporal images were classified using a decision tree (DT) algorithm (Figure 3). A DT is defined as a classification procedure that recursively partitions a data set into more uniform subdivisions based on tests defined at each node in the tree (Quinlan, 1993). A DT is composed of a root node, a set of internal nodes and a set of terminal nodes. Each internal node has one parent node and two or more descendant nodes.

A data set is classified according to the decision surfaces defined by the tree, and class labels are assigned to each observation according to the leaf node into which the observation falls. Decisions trees share advantages compared with traditional probabilistic algorithms because they are strictly nonparametric, free from distribution assumptions, able to deal with nonlinear relations, insensitive to missing values and capable of handling numerical and categorical inputs (Carvalho, 2001).

The classifier was trained with a set of sampled pixels (1500) distributed over seven main land cover types: cerrado, semideciduous and deciduous forest, water and others (eucalyptus, cultures and pasture).

To compare the classified images an accuracy assessment using an independent validation set of 1500 pixels was carried out based on the overall and per class accuracy as well as on the kappa coefficient. The validation set was based on field campaigns.

Error matrices are very effective representations of map accuracy because the individual accuracies of each map category with both the errors of inclusion and errors of exclusion (Congalton & Green, 1999).

3 RESULTS AND DISCUSSION

The results showed agreement between the vegetation indices and the monthly precipitation pattern. The seasonal behavior of the vegetation, which is mainly driven by precipitation, is clearly seen in the NDVI and EVI temporal profiles during the three years (Figure 4).

High NDVI and EVI values, indicative of high photosynthetic activity and biomass accumulation were found in the rainy months, while the lowest values in the dry period.

Similar results were found by Espig et al. (2006) using NDVI and EVI images for the year 2003 and 2004 working in a semiarid region of Brazil. They studied the seasonal variation of six areas and reported that the highest values of NDVI and EVI occurred in the months of higher precipitation.

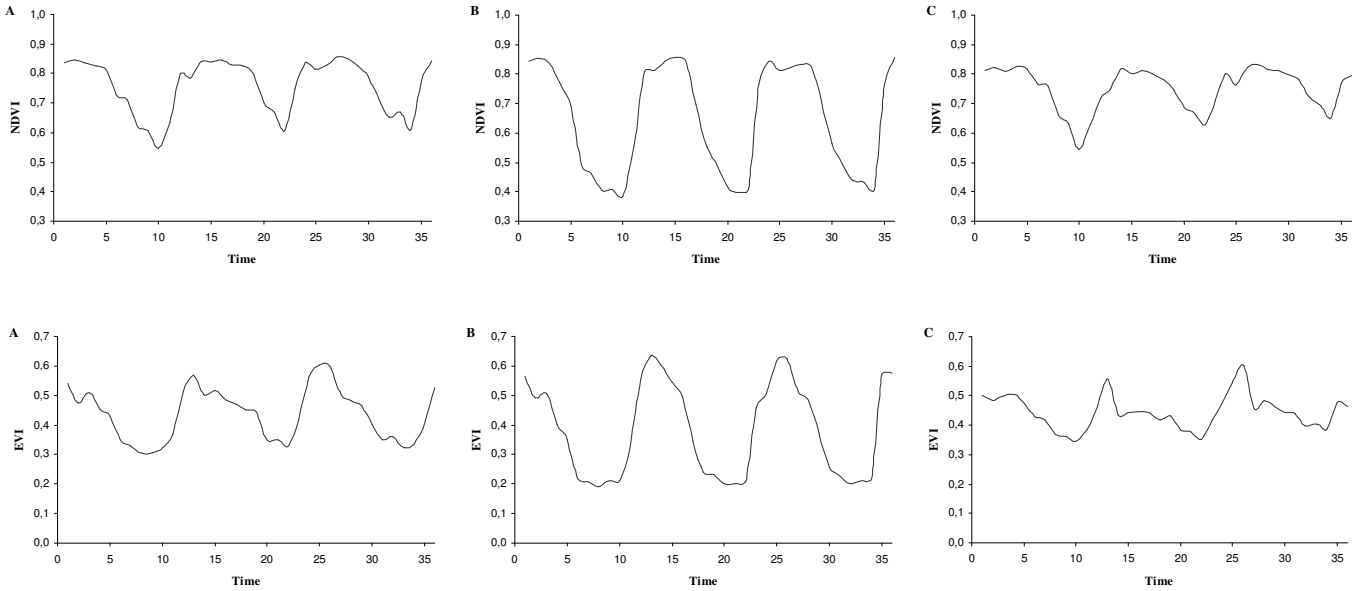

Figure 4 – NDVI and EVI temporal profiles for (A) cerrado, (B) deciduous forest and (C) semideciduous forest.

Figura 4 *– Perfil temporal dos índices NDVI e EVI para (A) cerrado, (B) floresta estacional decidual, (C) floresta estacional semidecidual.*

Xiao et al. (2006) conducted a regional scale analysis of tropical evergreen forests in South America using time series of EVI from MODIS in 2002 and the results shown a large dynamic range and spatial variations of annual maximum EVI The maximum EVI in 2002 typically occurs during the late dry season to early wet season. This suggest that leaf phenology in tropical evergreen forests is not determined by the seasonality of precipitation.

Among the vegetation types the deciduous forest showed the lowest VI values and the highest variation. This is because more than 50% of the leaves are lost during the dry season. These characteristics are consistent and distinct in comparison with other land cover types, and may provide valuable information that could potentially be used when classifying land cover types.

Compared to the deciduous forest the cerrado and the semideciduous forest presented higher VI values and lower variation. This is because most of the species in the cerrado are evergreen or semideciduous. Thus, leaf fall proceeds simultaneously with the development of new leaves and the total green biomass may decrease during the dry period, but the trees never remain entirely leafless.

According to Ferreira et al. (2004) there is a low overall range in VI values among the physiognomies, and this can be readily attributed to the narrow radiometric variations associated with the different land cover types. Near infrared variation among the physiognomies were low and thus, the EVI,

which by design tends to be more sensitive to NIR reflectances (Huete et al., 1997), yielded lower responses and variations.

The NDVI showed higher values than the EVI. This occurred because the EVI is sensitive to shadows and may be responding to the higher amount of shadows in the land cover types. The NDVI, by contrast, tends to be higher with shaded backgrounds (Ferreira et al., 2004).

Considering the classified images, in terms of overall accuracy and kappa coefficient the values were 89.9% and 0.86 for maps produced from NDVI images (Table 1), and 87.8% and 0.82 for maps produced from EVI images (Table 2). Based on these values the best vegetation index for mapping the vegetation classes in the study area was obtained using the NDVI images.

Table 1– Accuracy measures for maps produced from NDVI.

Tabela 1*– Medidas de acuracidade da classificação obtida através do NDVI*

Mapped class	Cerrado	Semideciduous	Deciduous	Commission error	User accuracy
Cerrado	90.2	22.0	3.3	9.4%	90.6 %
Semideciduous	6.6	75.0	0.0	21.0 %	78.9 %
Deciduous	0.0	0.0	89.6	1.1 %	98.9 %
Omission error	9.8 %	25.0 %	10.3 %		
Producer accuracy	90.2 %	75.0 %	89.7 %		
Overall accuracy	89.9 %	Kappa coefficient = 0.86			

Analysing the error matrix 90.2 % of the cerrado class areas have been correctly identified as cerrado and 90.6 % of the areas called cerrado on the map are actually cerrado on the ground.

Considering the deciduous class, 89.6 % of this class was correctly identified and 98.9% of the areas on the map are deciduous forest on the ground. For semideciduous class, 75.0% of this class area has been correctly identified and 78.9 % of the areas called semideciduous are actually semideciduous on the ground.

Thus, considering the NDVI time series for classification, the user accuracy show higher values than the producer accuracy for all classes. As a result the classes areas were more excluded from the category to which they actually belong than included in an incorrect category.

Table 2 – Accuracy measures for maps produced from EVI .

Tabela 2 *– Medidas de acuracidade da classificação obtida através do EVI.*

Mapped class	Cerrado	Semideciduous	Deciduous	Commission error	User accuracy
Cerrado	92.0	12.5	9.7	10.4 %	89.6 %
Semideciduous	7.8	85.0	0.0	26.1 %	73.9 %
Deciduous	0.0	0.0	80.0	5.9 %	94.1 %
Omission error	8.0 %	15.0 %	20.0 %		
Producer accuracy	92.0 %	85.0 %	80.0 %		
Overall accuracy	87.8 %	Kappa coefficient = 0.82			

Considering the EVI time series for classification, the user accuracy show higher values than the producer accuracy only for the deciduous class. Thus considering the cerrado and semideciduous classes, the areas were more

included incorrectly than excluded from the classes to witch they belong. The inverse occurred with the deciduous class.

In both classifications, the higher commission error values were encountered for semideciduous class. The higher omission error values were encountered for semideciduous class for NDVI (25.0%) and deciduous class (20.0%) for EVI.

The classified NDVI and EVI images are shown in Figure 5. Comparing the classified images, the shape and spatial location of the classes were well defined in both images. The highest misclassification value occurred between semideciduous and cerrado class.

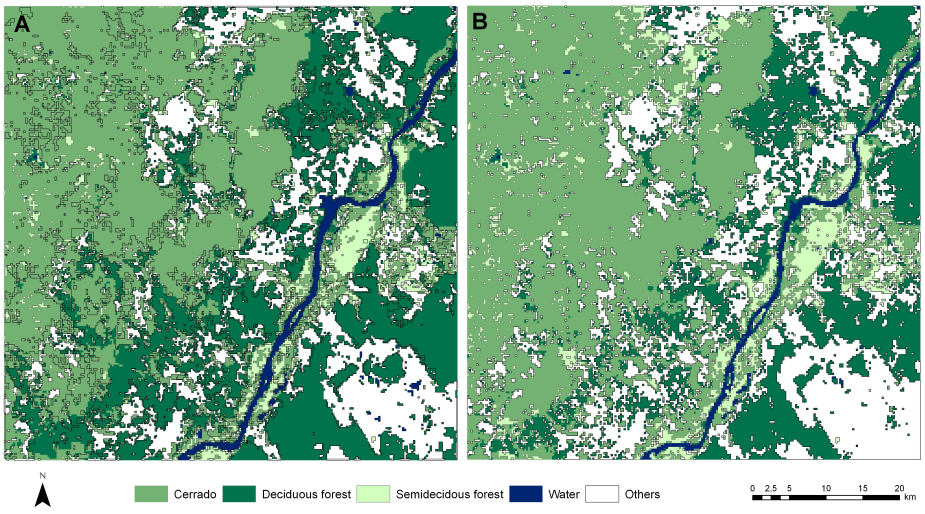

Figure 5 – Classified images – (A) NDVI (B) EVI.

Figura 5 *– Imagens classificadas - (A) NDVI (B) EVI.*

4 CONCLUSIONS

We evaluated the seasonal dynamics of cerrado, deciduous and semideciduous forest in the north of Minas Gerais, Brazil, using time series of NDVI and EVI derived from MODIS.

As a conclusion the vegetation indices temporal profiles were efficient to depict the seasonal dynamics of vegetation showing an agreement with the monthly precipitation pattern. The best index for mapping cerrado, deciduous and semideciduos forest in the study area is the NDVI. However both indices might be used to assess the vegetation seasonal dynamic.

After these promising results, further research need to be carried out exploring the use of feature extractions algorithms to improve classification accuracy of cerrado, semideciduous and deciduos forests in Minas Gerais, Brazil.

5 BIBLIOGRAPHICAL REFERENCES

ASRAR, G.; MYNENI, R.B.; KANEMASU, E.T. Estimation of plant canopy attributes from spectral reflectance measurements. In: ASRAR, G. **Theory and applications of optical remote sensing**. New York: J. Wiley, 1989. p.252–296.

BARET, F.; GUYOT, G. Potentials and limits of vegetation indices for LAI and APAR assessment. **Remote Sensing of Environment**, n.35, p.161–173, 1991.

CARVALHO, L.M.T. **Mapping and monitoring forest remnants**: a multiscale analysis of spatio-temporal data. 2001. 138p. Thesis (Doctor in Geoscience) – Wageningen University, Wageningen.

CONGALTON, R.G.G.; GREEN, K. **Assessing the accuracy of remotely sensed data:** principles and practices. New York: Lewis, 1999. 137p.

ESPIG, S.A.; SOARES, J.V.; SANTOS, J.R. Variações sazonais do EVI e NDVI em áreas do semi-árido brasileiro. In: SEMINÁRIO EM ATUALIZAÇÃO EM SENSORIAMENTO REMOTO E SISTEMAS DE INFORMAÇÕES GEOGRÁFICAS APLICADOS À ENGENHARIA FLORESTAL, 7., 2006, Curitiba. **Anais...** São José dos Campos: INPE, 2006. p.219-223.

FERREIRA, L.G.; YOSHIOKA, H.; HUETE, A.; SANO, E.E. Optical characterization of the Brazilian savanna phisiognomies for improved land cover monitoring of the cerrado biome: preliminary assessments from an airborne campaign over an LBA core site. **Journal of Arid Environments,** v.56, p.425-447, 2004.

FRASER, R.S.; KAUFMAN, Y.J. The relative importance of aerosol scattering and absorption in remote sensing. **IEEE Transactions on Geoscience and Remote Sensing**, n.23, p.625- 633, 1985.

HOLBEN, B.N. Characterization of maximum value composites from temporal AVHRR data. **International Journal of Remote Sensing,** v.7, p.1417-1434, 1986.

HUETE, A.; DIDAN, K.; MIURA, T.; RODRIGUEZ, E. Overview of the radiometric and biophysical performance of the MODIS vegetation indices. **Remote Sensing of Environment**, v.83, p.195–213, 2002.

HUETE, A.; JUSTICE, C.; LIU, H. Development of vegetation and soil indices for MODIS-EOS. **Remote Sensing of Environment**, n.49, p.224-234, 1994.

HUETE, A.R.; LIU, H.Q.; BATCHILY, K.; VAN LEEUWEN, W. A comparison of vegetation indices over a global set of TM images for EOS-MODIS. **Remote Sensing of Environment,** n.59, p.440-451, 1997.

HUETE, A.R.; JUSTICE, C.O.; VAN LEEUWEN, W. **MODIS vegetation index (MOD 13), EOS MODIS algorithm-theoretical basis document, NASA Goddard Space Flight Center.** Greenbelt: Maryland, 1991. 131p.

JUSTICE, C.O.; VERMOTE, E.; TOWNSHEND, J.R.G.; DEFRIES, R.; ROY, D.P.; HALL, D.K.; SALOMONSON, V.V.; PRIVETTE, J.L.; RIGGS, G.; STRAHLER, A.; LUCHT, W.; MYNENI, R.B.; KNYAZIKHIN, Y.; RUNNING, S.W.; NEMANI, R.R.; WAN, Z.M.; HUETE, A.R.; VAN LEEUWEN, W.; WOLFE, R.E.; GIGLIO, L.; MULLER, J.P.; LEWIS, P.; BARNSLEY, M.J. The moderate resolution imaging spectroradiometer (MODIS): land remote sensing for global change research. **IEEE Transactions on Geoscience and Remote Sensing**, n.36, p.1228–1249, 1997.

LILLESAND, T.M.; KIEFER, R.W. **Remote sensing and image interpretation.** New York: J. Wiley, 1987. 724p.

LILLESAETER, O. Spectral reflectance of partly transmitting leaves: laboratory measurements and mathematical modeling. **Remote Sensing of the Environment**, n.12, p.247–254, 1982.

LIU, H.Q.; HUETE, A.R. A feedback based modification of the NDVI to minimize canopy background and atmospheric noise. **IEEE Transactions on Geoscience and Remote Sensing**, v.33, p.457-465, 1995.

MYNENI, R.B.; KEELING, C.D.; TUCKER, C.J.; ASRAR, G.; NEMANI, R.R. Increased plant growth in the northern high latitudes from 1981–1991. **Nature,** v.386, p.698-702, 1997.

MUCHONEY, D.; BORAK, J.; CHI, H.; FRIEDL, M.; GOPAL, S.; HODGES, J.; MORROW, N.; STRAHLER, A. Application of the MODIS global supervised classi. cation model to vegetation and land cover mapping of Central America. **International Journal of Remote Sensing,** v.21, n.6/7, p.1115-1138, 2000.

QUINLAN, J. R. **Programs for machine learning**. Amsterdam: M. Kaufmann, 1993. 328p.

REED, B.C.; BROWN, J.F.; VANDERZEE, D.; LOVELAND, T.R.; MERCHANT, J.W.; OHLEN, D.O. Measuring phenological variability from satellite imagery. **Journal of Vegetation Science,** v.5, p.703-714, 1994.

SADER, S.A.; STONE, T.A.; JOYCE, A.T. Remote sensing of tropical forests: an overview of research and applications using no photographic sensors. **Photogrammetric Engineering and Remote Sensing**, v.56, p.1343–1351, 1990.

SCOLFORO, J.R.; CARVALHO, L.M.T. **Mapeamento e inventário da flora nativa e dos reflorestamentos de Minas Gerais.** Lavras: UFLA, 2006. 288p.

XIAO, X.; HAGEN, S.; ZHANG, Q.; KELLER, M.; MOORE, B. Detecting leaf phenology o seasonally moist tropical forests in south America with multi-temporal MODIS images. **Remote Sensing of Environment,** n.103**,** p.465–473, 2006.

ZHANG, X.; SOHLBERG, R.A.; TOWNSHEND, J.R.G.; DIMICELI, C.; CARROLL, M.L.; EASTMAN, J.C. Detection of land cover changes using MODIS 250 m data. **Remote Sensing of Environment**, n.83, p.336–350, 2002.

CHAPTER 03

MULTISCALE FEATURE EXTRACTION OF MODIS MULTITEMPORAL VEGETATION INDEX USING WAVELETS

Eduarda Martiniano de Oliveira Silveira[1], Luis Marcelo Tavares de Carvalho[1],

Fausto Weimar Acerbi-Júnior[1], José Marcio de Mello[1]

[1]Federal University of Lavras – UFLA - PO Box 3037 - 37200-000 - Lavras-MG, Brazil - dudalavras@hotmail.com; {passarinho; fausto; jmello}@ufla.br

(Prepared according to International Journal of Applied Earth Observation and Geoinformation - JAG)

Abstract: Temporal vegetation signatures generated using the MODIS imagery provide information about the phenological development of the vegetation types. In this study the use of NDVI time series and feature extraction algorithm to improve classification accuracy of cerrado, semideciduous and deciduous forests in Minas Gerais, Brazil was analyzed. In order to perform feature extraction the temporal signatures were transformed using the 1D version of the algorithm "à trous" with linear and cubic spline wavelets. After decomposition, the smoothed signatures were used as feature vectors in the classification process as well as the NDVI time series. The results demonstrated that wavelet decomposition increase the accuracy of the classification when the algorithm in the transformation is properly chosen as well as the level of decomposition. However, further studies should be done, using a wide variety of wavelets, in order to select the most appropriate type for each application and each land cover type.

Key-words: Time series; Vegetation indices; Feature extraction; Wavelets.

1 INTRODUCTION

The MODIS (MODerate resolution Imaging Spectroradiometer) sensor has been widely used in areas such as fire detection, water vapor column characterization, and burn scar analysis (Wang et al., 2003; Li et al., 2004). However, limited work has been done in the field of detailed vegetation classification using MODIS data.

Because of the synoptic coverage and repeated temporal sampling that satellites observation afford, remotely sensed data has significant potential for mapping and monitoring vegetation dynamics at regional to global scales (Mynemi et al., 1997). Additionally, MODIS provide frequent revisits, typically once every other day, and this can be the key for some studies.

Different types of vegetation have different temporal growth patterns. This will affect the characteristic shape of their NDVI (Normalized Difference Vegetation Index) temporal signatures. This can then be used to extract features that best discriminate different land cover types as well as to train a classifier (Bruce et al., 2006).

Since 1807, Fourier analysis has been the major technique used to represent signals in the frequency domain. Nevertheless, many of the signals analyzed do not have an appropriate representation using the Fourier Transform. This flaw representation occurred, mainly, because Fourier Transform does not provide good frequency localization in the time domain. The appropriate

localization is achieved by Wavelet Transform and this characteristic has brought good results.

Recently, Bruce et al. (2006) described the use of MODIS time series data for the detection of specific tropical invasive species vegetation types focusing on feature extraction methods. They concluded that the wavelet based feature extraction is significantly outperformed to improve classification accuracy.

Thus, this study was motivated by the following research question:

1. Can wavelet based feature extraction improve the classification accuracy in the study area?

The general objectives of this study were:

(1) To study the potential of the discrete wavelet transform in order to extract features to improve classification; (2) To investigate this method in order to separate different land cover types; (3) To compare the performance of feature extraction method to traditional methods;

2. METHODS

2.1 Study area and MODIS data

The study area (**Figure 1**) is located in the state of Minas Gerais, Brazil and is delimited by the coordinates S 14º 47’ 25.62’’ - S 15º 53’ 16.44” and W 43º 52’ 52.21’’ - W 45º 6’17.95’’. The area is covered by three major land cover types: deciduous forest, semideciduous forest and cerrado (Brazilian savannas).

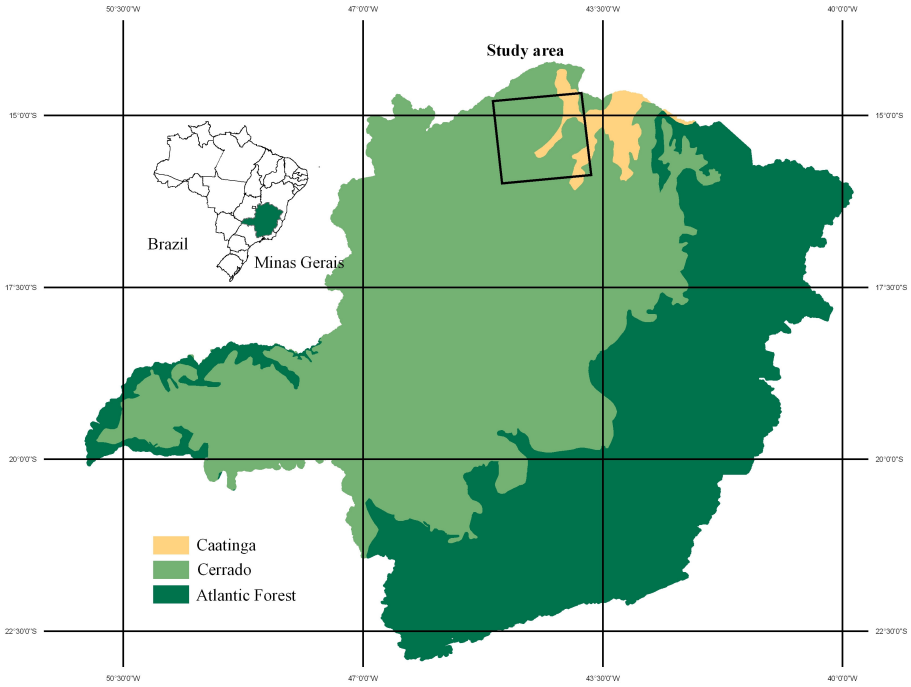

FIGURA 1: Study area.

MODerate resolution Imaging Spectroradiometer (MODIS) 16-day vegetation indices composite with 250 m of spatial resolution from TERRA

satellite, were used to derive three years (2003, 2004 and 2005) NDVI temporal profile.

The radiometric and geometric properties of MODIS sensor onboard NASA's Terra spacecraft, in combination with improved atmospheric correction and cloud screening, provide a substantially improved basis for monitoring vegetation dynamics (Zhang et al., 2002). The MODIS sensor has 36 spectral bands extending from the visible to the thermal infrared wavelengths, where seven bands are specifically designed for land applications with spatial resolutions ranging from 250 m to 1 km (Justice et al., 1997).

The spatial resolution of MODIS imagery varies depending on the type of data product. The product number 13 (MOD 13) is a land product that provides two gridded vegetation indices, normalized difference vegetation index (NDVI) and enhanced vegetation index (EVI). These indices give an estimate of the amount of vegetation on a ground pixel with spatial resolution of 250m by 250m.

The theoretical basis for empirical based vegetation indices is derived from examination of typical spectral reflectance signatures of leaves. The reflected energy in the visible is very low as a result of high absorption by photosynthetically active pigments with maximum sensitivity in the blue (470 nm) and red (670 nm) wavelengths. Nearly all of the near-infrared radiation is scattered (reflected and transmitted) with very little absorption, in a manner

dependent upon the structural properties of a canopy (LAI, leaf angle distribution, leaf morphology).

As a result, the contrast between red and near-infrared responses is a sensitive measure of vegetation amount, with maximum red - NIR differences occurring over a full canopy and minimal contrast over targets with little or no vegetation. For low and medium amounts of vegetation, the contrast is a result of both red and NIR changes, while at higher amounts of vegetation, only the NIR contributes to increasing contrasts as the red band becomes saturated due to chlorophyll absorption. (Huete et al., 1997).

Along with the image data, there exists a map that associates a quality assurance number (QA) with each pixel of the image. The QA is a 16 bit coded integer. The various groups of this 16 bit long binary code describe different properties of the pixel. One can set thresholds or specific values for these different groups to check the 'quality' of the pixel and then label it either good or bad depending upon the application.

The images were reprojected to Albers Conic Equal Area projection and the quality assessment (QA) was carried out through MODIS metadata in order to ensure that the images were generated without errors or artifacts.

The NDVI is a normalized transform of the NIR to red reflectance ratio, ρ nir/ρ red , designed to standardize VI values between –1 and +1 formulated as:

$$NDVI = \frac{\left[\left(\rho_{nir} / \rho_{red}\right) - 1\right]}{\left[\left(\rho_{nir} / \rho_{red}\right) + 1\right]} \qquad (1)$$

As a ratio, the NDVI has the advantage of minimizing certain types of band correlated noise (positively-correlated) and influences attributed to variations in direct/diffuse irradiance, clouds and cloud shadows, sun and view angles, topography, and atmospheric attenuation. Rationing can also reduce, to a certain extent, calibration and instrument-related errors (Huete et al., 1997).

2.2 Feature extraction

In order to perform feature extraction the temporal signatures were transformed using the 1D version of the algorithm "à trous" with linear and cubic spline wavelets (Holschneider et al., 1989; Carvalho, 2001).

Wavelet analysis mathematically approximates a data series by a linear combination of functions (wavelets) with specific scales (resolutions) and locations (positions along the data series). This transform provides a robust methodology for analysis in different scales. The wavelet transform allows for the decomposition of a signal using a series of elemental functions called wavelets and scaling function, which are created by scaling and translating a base function, known as the mother wavelet:

$$\psi_{s,u}(x) = \frac{1}{\sqrt{S}}\psi\left(\frac{x-u}{s}\right) \qquad (2)$$

where "*s*" governs the scaling and "*u*" the translation. The wavelet decomposition of a function is obtained by applying each of the basis functions or wavelets to the original function:

$$Wf(s,u) = \int_{\Re} f(x)\frac{1}{\sqrt{s}}\psi^{*}\left(\frac{x-u}{s}\right)dx \qquad (3)$$

Another point of view on the wavelet transform is by means of filter banks. In signal processing, a digital filter is a time invariant operator, which acts on an input vector, producing a transformed vector by means of mathematical convolution. Low pass and high pass filters are both considered in the wavelet transform, and their complementary use provides signal analysis and synthesis (Starck et al., 1998). The lowpass filter reduces the high frequency components keeping only the low frequency components of the signal and the highpass filter removes the low frequency components.

Part of the success of the wavelet transform is due to the existence of fast algorithms. A wavelet transform for discrete data might be provided by a procedure knows as the "à trous" algorithm (Hoslchneider et al., 1989; Shensa, 1992). The "à trous" algorithm represents a discrete approach to the classical continuous wavelet transform.

Using an algorithm as the "à trous" the decomposed signal has the same number of samples as the original signal and thus this wavelet transform is a redundant one. A redundant representation, which avoids signal decimation, has the same number of wavelet coefficients at all levels. When a dominant or significant feature appears at a given level, it should appear at successive levels. In contrast, a non-significant feature (i.e. noise) does not appear in next levels. It thus appears that a dominant feature is tied to its presence or duplication at successive levels.

Then, it is possible to follow the evolution of the wavelet decomposition from level to level, the algorithm produces a single wavelet coefficient plan at each level of decomposition and the wavelet coefficients are computed for each location allowing a better detection of a dominant feature and the algorithm is easily implemented (Chibani & Houacine, 2003).

The input signal is analyzed by using the coefficients of a properly chosen lowpass filter (Chui, 1992). The first approximation $\{c_0(k)\}$(at scale 0) which is the scalar product of the function $f(x)$ with the scaling function $\phi(x)$ (corresponding to an "*a trous*" lowpass filter H):

$$c_0(k) = f(x), \phi(x-k) \qquad (4)$$

The approximation of $f(x)$ at scale $i \geq 1$ is then performed by the direct "*à trous*" decomposition:

$$c_1(k) = \frac{1}{2^i}\left\langle f(x), \phi\left(\frac{x-k}{2^i}\right)\right\rangle \qquad (5)$$

The signal difference $\{c_0(k)\} - \{c_{i+1}(k)\}$ contains the information between two scales and is the discrete set associated with the wavelet transform corresponding to $\phi(x)$. The associated wavelet is therefore $\psi(x)$:

$$\psi(x) = \phi(x) - \frac{1}{2}\phi\left(\frac{x}{2}\right) \qquad (6)$$

The wavelet coefficients $w_i(k)$ are computed by:

$$w_i(k) = c_{i-1}(k) - c_i(k) \qquad (7)$$

The algorithm allowing one to rebuild the original signal is evident: the smoothed array c_{n_p} is added to all the differences w_i.

Figure 2 shows an example of a decomposition using the "à trous" algorithm.

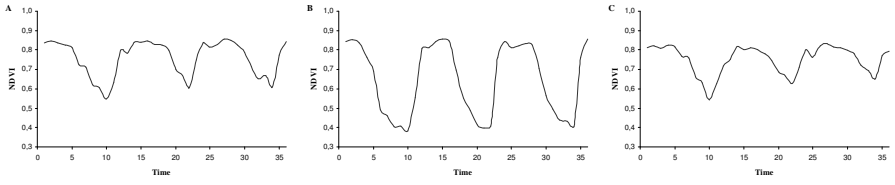

Original signature

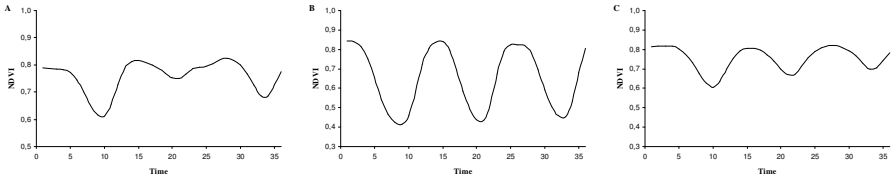

Smoothed signature with one decomposition level

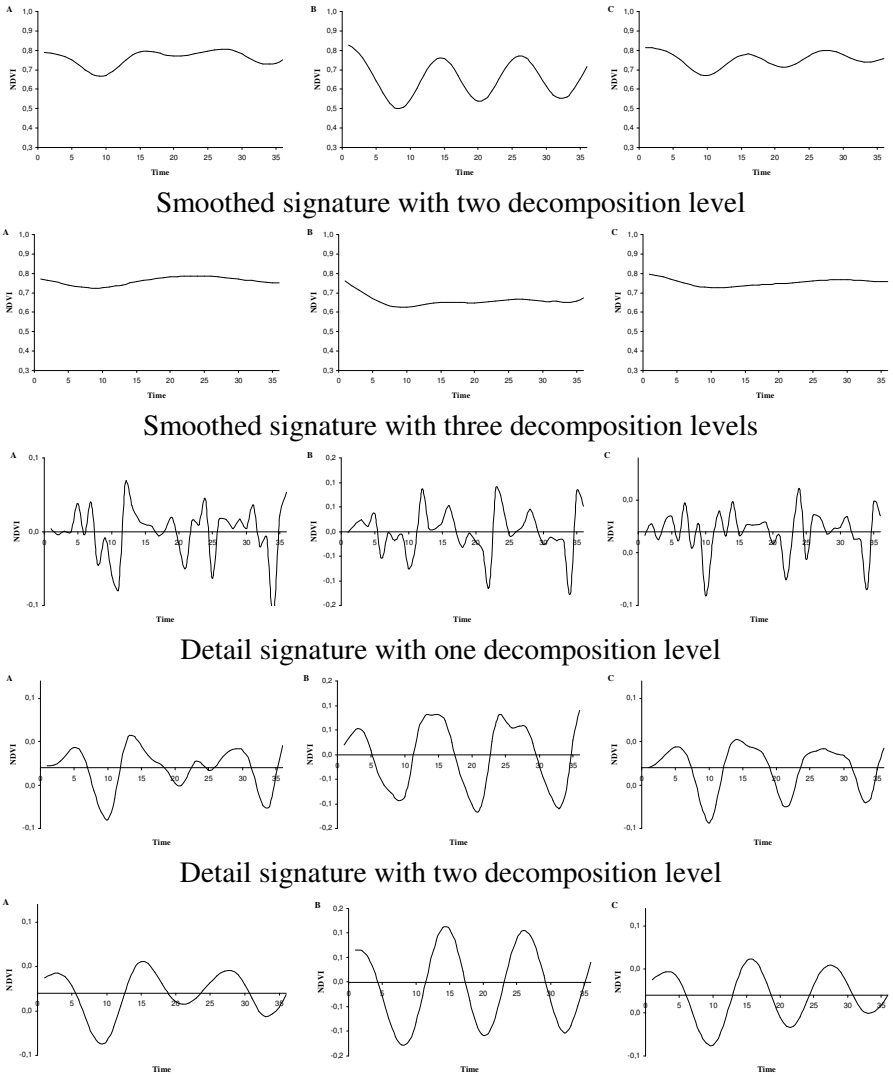

FIGURE 2. Decomposition using the“a trous” algorithm. Average NDVI temporal signatures for (A) cerrado, (B) deciduous forest and (C) semideciduous forest.

After decomposition, the smoothed signatures were used as feature vectors in the classification process. Seven feature sets were input to classification:

SET 01 – NDVI – Time series of NDVI –36 monthly NDVI images derived from MODIS sensor acquired yearly from 2003 till 2005.

SET 02 – LSO - First scale linear spline smoothed NDVI time series - 36 months of NDVI yearly from 2003 till 2005 were transformed using the "à trous" algorithm using a linear spline filter with one decomposition level.

SET 03 – LSW - Second scale linear spline smoothed NDVI time series - 36 months of NDVI yearly from 2003 till 2005 were transformed using the "à trous" algorithm using a linear spline filter with two decomposition levels.

SET 04 – LST - Third scale linear spline smoothed NDVI time series - 36 months of NDVI yearly from 2003 till 2005 were transformed using the "à trous" algorithm using a linear spline filter with three decomposition levels.

SET 05 – CSO - First scale cubic spline smoothed NDVI time series - 36 months of NDVI yearly from 2003 till 2005 were transformed using the "à trous" algorithm using a cubic spline filter with one decomposition level.

SET 06 – CSW - Second scale cubic spline smoothed NDVI time series - 36 months of NDVI yearly from 2003 till 2005 were transformed using the "à trous" algorithm using a cubic spline filter with two decomposition levels.

SET 07 – CST - Third scale cubic spline smoothed NDVI time series

- 36 months of NDVI yearly from 2003 till 2005 were transformed using the "à trous" algorithm using a cubic spline filter with three decomposition levels.

2.3 Classification procedure

The seven features sets were classified using a decision tree (DT) algorithm. A DT is defined as a classification procedure that recursively partitions a data set into more uniform subdivisions based on tests defined at each node in the tree. A DT is composed of a root node, a set of internal nodes and a set of terminal nodes. Each internal node in a DT has one parent node and two or more descendant nodes. A data set is classified according to the decision surfaces defined by the tree, and class labels are assigned to each observation according to the leaf node into which the observation falls (Quinlan, 1993).

Decision trees share advantages compared with traditional probabilistic algorithms because they are strictly nonparametric, free from distribution assumptions, able to deal with nonlinear relations, insensitive to missing values and capable of handling numerical and categorical inputs (Carvalho, 2001).

The classifier was trained with a set of sampled pixels (1500) distributed over seven main land cover types: cerrado, semideciduous and deciduous forest, water, eucalyptus, cultures and pasture. The last three classes were combined to generate the class others. The selection was based on field campaigns, as well as

on a vegetation map produced at the Federal University of Lavras (UFLA) (Scolforo & Carvalho, 2006).

To compare the classified images an accuracy assessment using an independent validation set of 1500 pixels was carried out based on the overall and per class accuracy as well as on the kappa coefficient. Error matrices are very effective representations of map accuracy because the individual accuracies of each map category is estimated from both the errors of comission and errors of omission (Congalton & Green, 1999).

3. RESULTS AND DISCUSSION

Considering the classification results, in terms of overall accuracy all the classified images presented values higher than 80% (Table 01). In terms of overall accuracy and kappa coefficient, the wavelet transform implemented with a linear spline filter and two decomposition levels (LSW) was the best technique (90.42%) as input for decision tree classification. The worst classification accuracy (81.04%) was provided by the wavelet transform implemented with a cubic spline filter and two decomposition levels (CSW).

Table 1 shows the classes accuracy measures for each technique tested.

TABLE 1. Overall accuracy and kappa coefficient

Techniques	Overall accuracy	kappa coefficient
NDVI	89.93%	0.86
LSO	86.32%	0.80
LSW	90.42%	0.87
LST	85.07%	0.79
CSO	81.60%	0.74
CSW	81.04%	0.73
CST	81.18%	0.74

In terms of per class accuracy, considering the LSO feature set, the user accuracy showed higher values than the producer accuracy for deciduous (96.54%) and semideciduous (94.44%) classes (Table 02). The cerrado class obtained better results considering the producer accuracy (91.33%).

Considering the LSW, LST, CSO and CSW feature sets the user accuracy showed higher values than the producer accuracy for all classes. Considering the CST feature set, the user accuracy showed higher values than the producer accuracy for cerrado and semideciduous classes. For the deciduous class, the inverse pattern was verified.

Considering all these classifications, the lower comission error for the cerrado class was obtained with LSW feature set (6.2%). For the deciduous class it was obtained with the original NDVI time series (1.1%). For the semideciduous class, the best classification result considering the commission error was obtained when using LSO feature set (5.56%).

Considering the omission errors, the better results were obtained when using the LSO feature set (8.67%), the original NDVI time series (10.33%) and LSW (11.5%), for cerrado, deciduous and semidecidous classes, respectively.

Similar results were found by Bruce et al. (2006) using the wavelet based features to increase the overall classification accuracy from 95% to 100% for two types of vegetation.

As for the choice of the best feature vector to classifier, decisions of what should be considered the best or worst in terms of accuracy depends on the objective of the mapping project as well as the classes. On this study the producer and user accuracy was chosen as indicator.

As a result, considering all the classified images but focusing only on the cerrado class the highest producer accuracy value (91.33%) was obtained using the LSO, however, considering the user accuracy, the best feature vector to classify this vegetation type was the LSW (93.80%). Therefore, a compromise choice to classify the cerrado areas would be to use the LSW feature set, since it presents the highest user accuracy and the second highest producer accuracy.

The best feature vector to classify the semideciduous class considering the producer accuracy was the LSW (88.50%) Considering the user accuracy, the best feature vector was the LSO (94.44%). Again, the compromise choice would be to select the LSW feature set, since it presents the highest producer accuracy and the second highest user accuracy.

The best feature vector to classify the deciduous class considering the producer and user accuracy was the original NDVI time series (89.67% and 98.90%).

Table 02 shows an overview of the results for each technique tested and each vegetation type.

TABLE 2. Accuracy measures for maps produced

Cerrado	LSO	LSW	LST	CSO	CSW	CST	NDVI
Comission Errors (%)	13.43	6.20	9.30	14.55	12.81	11.63	9.38
Omission Errors (%)	8.67	9.17	15.50	15.83	17.17	24.00	9.83
Producer's accuracy (%)	91.33	90.83	84.50	84.17	82.83	76.00	90.17
User's accuracy (%)	86.67	93.80	90.70	85.45	87.19	88.37	90.62
Deciduous	**LSO**	**LSW**	**LST**	**CSO**	**CSW**	**CST**	**NDVI**
Comission Errors (%)	3.46	5.47	15.60	3.91	4.47	26.47	1.10
Omission Errors (%)	16.33	13.67	17.00	26.33	21.67	16.67	10.33
Producer's accuracy (%)	83.67	86.33	83.00	73.67	78.33	83.33	89.67
User's accuracy (%)	96.54	94.53	84.40	96.09	95.53	73.53	98.90
Semideciduous	**LSO**	**LSW**	**LST**	**CSO**	**CSW**	**CST**	**NDVI**
Comission Errors (%)	5.56	7.81	18.60	31.28	25.00	17.74	21.05
Omission Errors (%)	40.50	11.50	23.50	28.50	35.50	23.50	25.00
Producer's accuracy (%)	59.50	88.50	76.50	61.50	64.50	76.50	75.00
User's accuracy (%)	94.44	92.19	81.40	68.72	75.00	82.26	78.95

4. CONCLUSIONS

This study demonstrated the importance of wavelet transform to extract features of temporal signatures to produce accurate maps. It was demonstrated that wavelet decomposition improves land cover classification accuracy when the algorithm used in the transformation and the levels are properly chosen. Thus, the choice of the best feature vector to classify is dependent on the objectives of the mapping projected.

However, further studies should be done, using a wide variety of wavelets, in order to select the most appropriate type for each application and each vegetation type on the study area.

5 BIBLIOGRAPHICAL REFERENCES

BRUCE, L.M.; MARTHUR, A.; BIRD JR, J.D. Denoising and wavelet-based feature extraction of MODIS multi-temporal vegetation signatures. **GIScience & Remote Sensing**, n.43, p.170-180, 2006.

CARVALHO, L.M.T. **Mapping and monitoring forest remnants**: a multiscale analysis of spatio-temporal data. 2001. 138p. Thesis (Doctor in Geoscience) – Wageningen University, Wageningen.

CHUI,C.K. **An introduction to wavelets**. San Diego, CA: Academic, 1992.

CHIBANI, Y.; HOUACINE, A. Multiscale versus multiresolution analysis for multisensor image fusion. **Proceedings of the European Signal Processing Conference**, Island of Rhodes, Greece, p.451–454, 2003.

CONGALTON, R.G.G.; GREEN, K. **Assessing the accuracy of remotely sensed data:** principles and practices. New York: Lewis, 1999. 137p.

HOLSCHNEIDER, M.; KRONLAND-MARTINET, R.; MORLET, J.; TCHMITCHIAN, P. A real time algorithm for signal analysis with the help of the wavelet transform. In: COMBES, J.M.; GROSSMAN, A.; TCHMITCHIAN, P. (Ed.). **Wavelets:** time frequency methods and phase space. New York: Springer-Verlag, 1989. p.286-297.

HUETE, A.R.; LIU, H.Q.; BATCHILY, K.; VAN LEEUWEN, W. A comparison of vegetation indices over a global set of TM images for EOS-MODIS. **Remote Sensing of Environment**, n.59, p.440– 451, 1997.

JUSTICE, C.O.; VERMOTE, E.; TOWNSHEND, J.R.G.; DEFRIES, R.; ROY, D.P.; HALL, D.K.; SALOMONSON, V.V.; PRIVETTE, J.L.; RIGGS, G.; STRAHLER, A.; LUCHT, W.; MYNENI, R.B.; KNYAZIKHIN, Y.; RUNNING, S.W.; NEMANI, R.R.; WAN, Z.M.; HUETE, A.R.;VAN LEEUWEN, W.; WOLFE, R.E.; GIGLIO, L.; MULLER, J.P.; LEWIS, P.; BARNSLEY, M.J. The moderate resolution imaging spectroradiometer (MODIS): land remote sensing for global change research. **IEEE Transactions on Geoscience and Remote Sensing**, n.36, p.228–249, 1997.

LI, R.R.; KAUFMAN, Y.J.; HAO, W.M.; SALMON, J.M.; GAO, B. A technique for detecting burn scars using MODIS data. **IEEE Transactions on Geoscience and Remote Sensing**, n.42, p.1300–1308, 2004.

MYNENI, R.B.; KEELING, C.D.; TUCKER, C.J.; ASRAR, G.; NEMANI, R.R. Increased plant growth in the northern high latitudes from 1981–1991. **Nature**, n.386, p.698–702, 1997.

QUINLAN, J.R. **Programs for machine learning**. Amsterdam: M. Kaufmann, 1993. 328p.

SCOLFORO, J.R.; CARVALHO, L.M.T. **Mapeamento e inventário da flora nativa e dos reflorestamentos de Minas Gerais**. Lavras: UFLA, 2006. 288p.

SHENSA, M.J. The discrete wavelet transform: wedding the a trous and Mallat algorithms. **IEEE Trans. Signal Process**, n.40, p.2464–2482, 1992.

STARCK J.L.; MURTAGH, F.; BIJAOUI, A. **Image processing and data analysis**. Cambridge: Cambridge University, 1998. 286p.

ZHANG, X.; SOHLBERG, R.A.; TOWNSHEND, J.R.G.; DIMICELI, C.; CARROLL, M.L.; EASTMAN, J.C. Detection of land cover changes using MODIS 250 m data. **Remote Sensing of Environment**, n.83, p.336–350, 2002.

WANG, S.; ZHOU, Y.; WANG, L.; ZHANG, P. A research on fire automatic recognition using MODIS data. **Proceedings of 2003 International Geoscience and Remote Sensing Symposium IGARSS**, n.4, p.2502–2504, 2003.

CHAPTER 04

MULTISENSOR IMAGE FUSION AND MULTISCALE FEATURE EXTRACTION ON CLASSIFICATION ACCURACY

Eduarda Martiniano de Oliveira Silveira[1], Fausto Weimar Acerbi-Júnior[1], Luis Marcelo Tavares de Carvalho[1].

[1]Federal University of Lavras – UFLA - PO Box 3037 - 37200-000 - Lavras-MG, Brazil - dudalavras@hotmail.com

(Prepared according to the International Journal of Remote Sensing)

ABSTRACT

SILVEIRA, Eduarda Martiniano de Oliveira. **Mappinf forests**: a mutiltemporal analysis. 2007. 150 p. Dissertação (Mestrado em Manejo Ambiental) – Universidade Federal de Lavras, Lavras, MG.[3]

The objectives of this paper were: (1) To assess the potential of using fused images between MODIS and TM images to improve classification accuracy; (2) To assess the potential of using fused images combined with feature extraction algorithms in order to improve image classification. In the multisensor image process, the source image consist of one NDVI obtained by Landsat TM image acquired on July, 2005 and a 36 monthly NDVI images derived from MODIS sensor acquired yearly from 2003 till 2005. The NDVI Landsat TM was decomposed by the pyramidal in Fourier space (PFS) wavelet transform. In order to perform feature extraction the temporal signatures were transformed using the 1D version of the algorithm "à trous" with linear and cubic spline wavelets. After decomposition, the smoothed signatures were used as feature vectors in the classification process. The Time series of NDVI as well as fused images and smoothed NDVI fused images were classified using a decision tree (DT) algorithm. The proposed data fusion and feature extraction method performed well in terms of overall accuracies as compared to results obtained by the original time series of NDVI.

[3] Comitê orientador: Luis Marcelo Tavares de Carvalho – UFLA (Orientador); Fausto Weimar Acerbi Junior – UFLA (Co-orientador).

1 INTRODUCTION

Many approaches have been developed to combine complementary information coming from input images in order to create a new image where the informative content is more suitable for human perception. The new composite image is produced according to a process called image fusion (Chibani & Houacine, 2003).

The wavelet decomposition has become an attractive tool for fusing multisensor images. Usually, the input images are decomposed with an orthogonal wavelet in order to extract features, which are combined through an appropriate fusion rule. The fused image is then reconstructed by applying the inverse wavelet transform.

Some examples include the fusion of Landsat TM (MS) and SPOT (P) images, SPOT (XS) and SPOT (P) images, and IKONOS (MS) and IKONOS (P) images (Núñes et al., 1999; Aiazzi et al., 2002; Ranchin et al., 2003).

More recently, pyramid schemes based on the wavelet transform have led many authors (Chapman & Orr, 1995; Wilson et al., 1995; Acerbi-Junior et al., 2006) to define more complicated fusion rules in order to improve the quality of the fused image.

For example, Acerbi-Junior et al (2004) demonstrated the efficiency of the pyramidal wavelet transform in Fourier space (PFS) wavelet transform to perform the fusion between MODIS (MODerate resolution Imaging

Spectroradiometer) and TM (Thematic Mapper) images. The Landsat TM imagery (30m) offers a good spatial resolution whereas MODIS imagery (250m) is a good means to capture most of the vegetation dynamics due to its high temporal resolution.

Since the 1970s, researches have recognized the potential of multitemporal satellite observations to provide information about the phenological development of natural vegetation and crops (Reed et al., 1994) moreover the combination of vegetation indices with multitemporal imagery that captures phenology has produced successful vegetation classifications (Sader et al., 1990).

According to Bruce et al (2006), different types of vegetation have different temporal growth patterns and this will affect the characteristic shape of their NDVI (Normalized Difference Vegetation Index) temporal signatures. This can then be used to extract features that best discriminate different land cover types as well as to train a classifier.

Thus, long time series combined with feature extractions algorithms and image fusion can be used to improve the separation of spectrally similar objects and produce accurate maps.

The objectives of this paper were; (1) To assess the potential of using fused images between MODIS and TM images to improve classification

accuracy; (2) To assess the potential of using fused images combined with feature extraction algorithms in order to improve image classification.

2 METHODS

2.1 Study area

The study area (Figure 1) is located in the state of Minas Gerais, Brazil and is delimited by the coordinates S 14º 47’ 25.62’’ - S 15º 53’ 16.44” and W 43º 52’ 52.21’’ - W 45º 6’17.95’’. The area is cover by three major land cover types: deciduous forest, semideciduous forest and cerrado (Brazilian savannas).

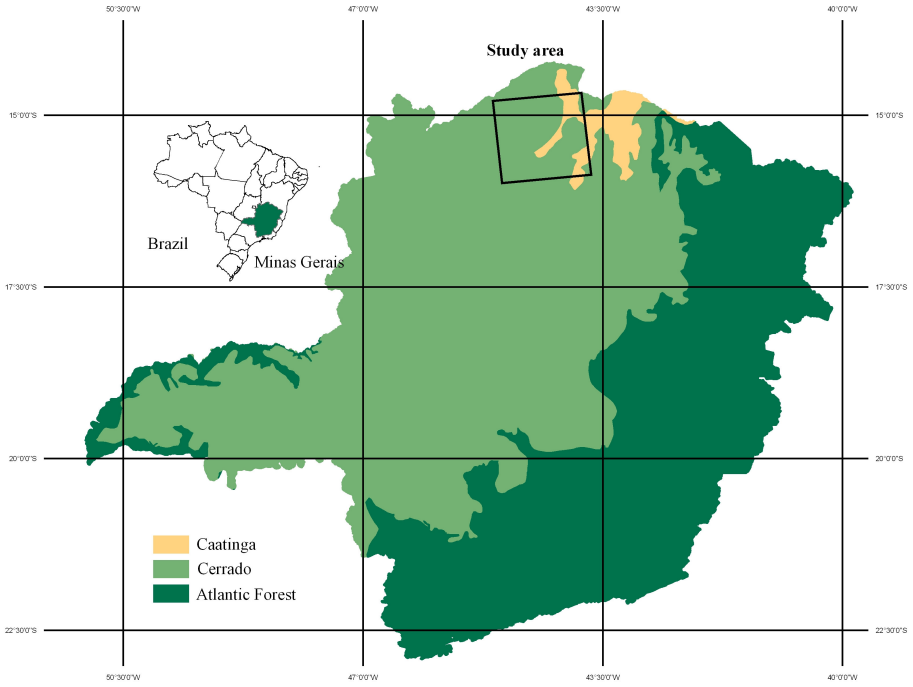

Figure 1 – Study area.

2.2 Data

MODerate resolution Imaging Spectroradiometer (MODIS) 16-day vegetation indices composite with 250 m of spatial resolution from TERRA satellite, were used to derive three years (2003, 2004 and 2005) NDVI time series.

In the multisensor image fusion process, the source image consisted of one NDVI obtained from Landsat TM image acquired on July 2005 and a 36 monthly NDVI images derived from MODIS sensor acquired yearly from january 2003 till december 2005.

The radiometric and geometric properties of MODIS sensor onboard NASA's Terra spacecraft, in combination with improved atmospheric correction and cloud screening, provide a substantially improved basis for monitoring vegetation dynamics (Zhang et al., 2002). The MODIS sensor has 36 spectral bands extending from the visible to the thermal infrared wavelengths, where seven bands are specifically designed for land applications with spatial resolutions ranging from 250 m to 1 km (Justice et al., 1997).

The spatial resolution of MODIS imagery varies depending on the type of data product. The product number 13 (MOD 13) is a land product that provides two gridded vegetation indices, normalized difference vegetation index (NDVI) and enhanced vegetation index (EVI). These indices give an estimated

of the amount of vegetation on a ground pixel with spatial resolution of 250m by 250m.

The theoretical basis for empirical based vegetation indices is derived from examination of typical spectral reflectance signatures of leaves. The reflected energy in the visible is very low as a result of high absorption by photosynthetically active pigments with maximum sensitivity in the blue (470 nm) and red (670 nm) wavelengths. Nearly all of the near-infrared radiation is scattered (reflected and transmitted) with very little absorption, in a manner dependent upon the structural properties of a canopy (LAI, leaf angle distribution, leaf morphology).

As a result, the contrast between red and near-infrared responses is a sensitive measure of vegetation amount, with maximum red - NIR differences occurring over a full canopy and minimal contrast over targets with little or no vegetation. For low and medium amounts of vegetation, the contrast is a result of both red and NIR changes, while at higher amounts of vegetation, only the NIR contributes to increasing contrasts as the red band becomes saturated due to chlorophyll absorption. (Huete et al., 1997).

Along with the image data, there exists a map that was used in order to associate a quality assurance number (QA) to each pixel of the image. The QA is a 16 bit coded integer. The various groups of this 16 bit long binary code describe different properties of the pixel. One can set thresholds or specific

values for these different groups to check the 'quality' of the pixel and then label it either good or bad depending upon the application.

2.3 Fusion procedure

To perform the fusion procedure the NDVI time series were resampled from 250 to 240 m and matched to the histogram of the Landsat TM NDVI image using linear scaling (Pohl, 1996). The aim was to normalize the mean and standard deviation between the images.

In order to match the spatial resolution of the NDVI MODIS images, the NDVI Landsat TM image was decomposed three levels using the pyramidal wavelet transform in Fourier space (PFS).

The PFS is a wavelet transform with a scaling function in Fourier space. Working in Fourier space, one can define a wavelet function from scaling functions at two different scales which is very appropriate for capturing useful scale related properties during the decomposition process (essentially relationships between neighboring pixels, as expressed by the frequency information in the Fourier transform (Starck et al, 1998; Acerbi Junior et al., 2006). PFS was selected based on its good performance obtained in a study which demonstrated the efficiency of this transform to perform fusion between MODIS and TM images (Acerbi-Junior et al., 2006).

The approximation images were replaced by the corresponding MODIS image and finally the process was inverted in order to reconstruct the fused images.

2.4 Quality assessment

Quality assessment of the fused images is important when they are used for classification. Classification process depends on the spectral information and any error in the synthesis of the spectral content of a fused image will result in classification errors (Meenakshisundaram & Couloigner, 2004).

The quality assessment approaches, the basic premise is to establish some measures to assess image quality. The quality assessment was based on qualitative and quantitative measures and they were associated to two types of criteria. The first type of criteria is related to the quality of the spectral information of a fused image. The second type of criteria is based on the quality of the spatial information of a fused image. It is strongly associated to the preservation of the spatial features throughout the fusion process.

The qualitative measure was derived from the visual judgment, comparing each fused image, according to their spatial similarity with the original NDVI TM image. Quantitative measures were applied to quantify the spectral differences between each fused image and the NDVI MODIS image. First the bias of the mean and variance per data were calculated based on the

mean and variance difference between the MODIS images and the fused images. Second, the root mean square error (RMSE) between the MODIS image and each fused image was calculated using a pixel based comparison.

2.5 Feature extraction

In order to perform feature extraction the temporal signatures were transformed using the 1D version of the algorithm "à trous" with linear and cubic spline wavelets (Holschneider et al., 1989; Carvalho, 2001).

Wavelet analysis mathematically approximates a data series by a linear combination of functions (wavelets) with specific scales (resolutions) and locations (positions along the data series). This transform provides a robust methodology for analysis in different scales. The wavelet transform allows for the decomposition of a signal using a series of elemental functions called wavelets and scaling function, which are created by scaling and translating a base function, known as the mother wavelet.

Another point of view on the wavelet transform is by means of filter banks. In signal processing, a digital filter is a time invariant operator, which acts on an input vector, producing a transformed vector by means of mathematical convolution. Low pass and high pass filter are both considered into the wavelet transform, and their complementary use provides signal analysis and synthesis (Starck et al., 1998). The lowpass filter reduces the high frequency

components keeping only the low frequency components of the signal and the highpass filter removes the low frequency components.

Part of the success of the wavelet transform is due to the existence of fast algorithms. A wavelet transform for discrete data might be provided by the "à trous" algorithm (Hoslchneider et al., 1989; Shensa, 1992). The "à trous" algorithm represents a discrete and redundant approach to the classical continuous wavelet transform.

A redundant representation, which avoids image decimation, has the same number of wavelet coefficients at all levels. When a dominant or significant feature appears at a given level, it should appear at successive levels. In contrast, a non-significant feature, i.e. noise, does not appear in the next levels. It thus appears that a dominant feature is tied to its presence or duplication at successive levels.

Then, it is possible to follow the evolution of the wavelet decomposition from level to level, the algorithm produces a single wavelet coefficient plan at each level of decomposition and the wavelet coefficients are computed for each location allowing a better detection of a dominant feature and the algorithm is easily implemented (Chibani & Houacine, 2003).

After decomposition, the smoothed signatures were used as feature vectors in the classification process. Seven feature sets were input to classification:

SET 01 – Original Time series of NDVI – 36 monthly NDVI images derived from MODIS sensor.

SET 02 – Time series of NDVI fused images – 36 monthly NDVI images derived from the fused images.

SET 03 – FLSO - First scale linear spline smoothed NDVI fused images time series - 36 months of NDVI derived from the fused images were transformed using the "à trous" algorithm using a linear spline filter with one decomposition level.

SET 04 – FLSW - Second scale linear spline smoothed NDVI fused images time series - 36 months of NDVI derived from the fused images were transformed using the "à trous" algorithm using a linear spline filter with two decomposition levels.

SET 05 – FLST - Third scale linear spline smoothed NDVI fused images time series - 36 months of NDVI derived from the fused images were transformed using the "à trous" algorithm using a linear spline filter with three decomposition levels.

SET 06 – FCSO - First scale cubic spline smoothed NDVI fused images time series - 36 months of NDVI yearly from 2003 till 2005 were transformed using the "à trous" algorithm using a cubic spline filter with one decomposition level.

SET 07 – FCSW - Second scale cubic spline smoothed NDVI fused images time series - 36 months of NDVI derived from the fused images were transformed using the "à trous" algorithm using a cubic spline filter with two decomposition levels.

SET 08 – FCST - Third scale cubic spline smoothed NDVI fused images time series - 36 months of NDVI derived from the fused images were transformed using the "à trous" algorithm using a cubic spline filter with three decomposition levels.

2.6 Classification procedure

The Time series of NDVI as well as fused images and smoothed NDVI fused images were classified using a decision tree (DT) algorithm. A DT is defined as a classification procedure that recursively partitions a data set into more uniform subdivisions based on tests defined at each node in the tree (Quinlan, 1993). A DT is composed of a root node, a set of internal nodes and a set of terminal nodes. Each internal node has one parent node and two or more descendant nodes. A data set is classified according to the decision surfaces defined by the tree, and class labels are assigned to each observation according to the leaf node into which the observation falls. Decisions trees share advantages compared with traditional probabilistic algorithms because they are strictly nonparametric, free from distribution assumptions, able to deal with

nonlinear relations, insensitive to missing values and capable of handling numerical and categorical inputs (Carvalho, 2001).

The classifier was trained with a set of sampled pixels distributed over seven main land cover types: cerrado, semideciduous and deciduous forest, water and others (eucalyptus, cultures and pasture). To evaluate the classified images an accuracy assessment was carried out based on the overall and per class accuracy as well as on the kappa coefficient. Error matrices are very effective representations of map accuracy because the individual accuracies of each map category with both the errors of inclusion and errors of exclusion (Congalton &Green, 1999).

3 RESULTS AND DISCUSSION

3.1 Quality assessment

The visual judgment between the TM image and fused image have shown that the size, shape and location of the spatial features were considered unchanged and the spectral content was considered to be similar to the MODIS image. Small spatial structures were not visible on the MODIS image but they were visible on the fused image, which means that small vegetation patches that were not detected due to MODIS spatial resolution can now be assessed using the fused images.

The results calculated by using the mean, standard deviation and the root mean square error (RMSE) as a quantitative measure (Table 01) comply with the results obtained from de visual judgment. These measures were selected in order to evaluate the similar spectral information and the spatial information since they show the similarity at pixel level between the MODIS image and the fused images.

The mean values for all fused images are identical to the mean values of the original MODIS images, which is expected since the wavelet coefficients have mean values around zero. The standard deviation values are measures of the quantity of spectral information added or lost during a fusion process. For all fused images the standard deviation values are similar to the standard deviation values of the MODIS original images, which demonstrates the good

performance of the fusion algorithm. The RMSE is another measure of similarity among the fused and the MODIS images, since all images presented values close to zero.

Based on these quantitative measures as well as on the visual judgment, one can say that the fused images are of good quality and can, therefore, be used for mapping and monitoring the vegetation dynamics.

Table 1. Statistcs of the fused images.

2003	Mean		Standard deviation		RMSE	2004	Mean		Standard deviation		RMSE	2005	Mean		Standard deviation		RMSE
	Fusão	MODIS	Fusão	MODIS			Fusão	MODIS	Fusão	MODIS			Fusão	MODIS	Fusão	MODIS	
Jan	0.781214	0.781214	0.096306	0.094456	0.062751	**Jan**	0.758471	0.758471	0.118036	0.122016	0.087178	**Jan**	0.742355	0.742355	0.108854	0.104724	0.067794
Feb	0.779549	0.779549	0.102091	0.09923	0.065381	**Feb**	0.771181	0.771181	0.136808	0.133972	0.087803	**Feb**	0.740529	0.740529	0.157716	0.157816	0.107929
Mar	0.754012	0.754012	0.106167	0.103562	0.068942	**Mar**	0.781832	0.781832	0.10797	0.104775	0.068971	**Mar**	0.780843	0.780843	0.104785	0.100723	0.064807
Apr	0.721803	0.721803	0.091469	0.087761	0.057409	**Apr**	0.775631	0.775631	0.098172	0.094559	0.061756	**Apr**	0.741399	0.741399	0.100348	0.095733	0.061761
May	0.682263	0.682263	0.103278	0.097643	0.062809	**May**	0.704811	0.704811	0.115884	0.107944	0.067725	**May**	0.678149	0.678149	0.116217	0.107855	0.067420
Jun	0.558148	0.558148	0.126918	0.115479	0.069533	**Jun**	0.631169	0.631169	0.140202	0.127331	0.076279	**Jun**	0.609677	0.609677	0.125334	0.11187	0.070383
Jul	0.528947	0.528947	0.130422	0.119008	0.071946	**Jul**	0.57984	0.57984	0.148682	0.134426	0.079729	**Jul**	0.740529	0.740529	0.157716	0.119611	0.070776
Aug	0.435768	0.435768	0.116133	0.10637	0.065069	**Aug**	0.491478	0.491478	0.139093	0.124739	0.072709	**Aug**	0.464598	0.464598	0.131014	0.117551	0.069002
Sep	0.447261	0.458461	0.151868	0.13615	0.063003	**Sep**	0.458339	0.458339	0.138137	0.124211	0.073089	**Sep**	0.477426	0.477426	0.133948	0.120305	0.070176
Oct	0.421778	0.421778	0.11396	0.10405	0.071506	**Oct**	0.458371	0.458371	0.151967	0.13628	0.079198	**Oct**	0.443056	0.443056	0.127286	0.115338	0.068506
Nov	0.511257	0.511257	0.111966	0.106014	0.066831	**Nov**	0.616991	0.616991	0.151365	0.139831	0.085207	**Nov**	0.640998	0.640998	0.1502051	0.143551	0.091215
Dec	0.685198	0.685198	0.142295	0.134042	0.084812	**Dec**	0.769383	0.769383	0.105783	0.100864	0.064466	**Dec**	0.749316	0.749316	0.140648	0.132721	0.082654

3.2 Classification procedure

In terms of overall accuracy all the classified images presented values higher than 80%. The highest overall accuracy value (95.41%) was reached using the second scale cubic spline smothed NDVI fused images as feature vector.

Decisions of what should be considered the best or worst in terms of accuracy depends on the objective of the mapping projected as well as the classes. Considering all the classified images but focusing only on the cerrado class the highest producer accuracy value (99.33%) was obtained using the third scale linear spline smothed NDVI time series. however. considering the user accuracy. the best feature vector to classify this vegetation type was the second scale cubic spline smothed NDVI fused images (100%) as well as time series of NDVI fused images (100%).v

The best feature vector to classify the deciduous class considering the producer accuracy was the second scale cubic spline smothed NDVI fused images (99.67%). however considering the user accuracy. the best feature vector was the first scale cubic spline smothed NDVI fused images (100%) or the first scale linear cubic smothed NDVI fused images (100%).

The best feature vector to classify the semideciduous class considering the producer accuracy was the first scale linear spline smothed NDVI fused images (86%) as well as the second scale cubic spline smothed NDVI fused

images (86%). Considering the user accuracy the best feature vector was the second scale cubic spline smothed NDVI fused images (87.31%).

Table 2 shows the classes accuracy measures for all the classified images.

Table 2. Accuracy measures.

Feature Vector	Error Matrix		Cerrado		Deciduous		Semideciduous	
	Overral Accuracy	Kappa Coefficent	Producer Accuracy	User Accuracy	Producer Accuracy	User Accuracy	Producer Accuracy	User Accuracy
Time series of NDVI	89.93	0.86	90.17	90.62	89.67	98.90	75.00	78.95
Time series of NDVI fused images	94.09	0.91	97.50	100.00	95.67	97.29	82.00	85.42
First scale linear spline smothed NDVI fused images	83.95	0.77	98.17	79.17	94.00	100.00	86.00	86.87
Second scale linear spline smothed NDVI fused images	89.30	0.85	96.67	99.83	98.67	82.91	71.50	81.25
Third scale linear spline smothed NDVI time series	92.50	0.89	99.33	97.07	98.67	83.08	81.00	83.94
First scale linear cubic smothed NDVI fused images	92.48	0.90	96.67	99.49	98.33	100.00	72.50	84.80
Second scale cubic spline smothed NDVI fused images	95.41	0.93	97.67	100.00	99.67	98.03	86.00	87.31
Third scale cubic spline smothed NDVI fused images	90.90	0.87	93.50	93.39	93.67	89.78	81.00	81.82

4 CONCLUSIONS

This study evaluated the potential of using fused images between MODIS and TM images to improve classification accuracy and the potential of using fused images combined with feature extraction algorithms in order to improve image classification.

The assessment of classification accuracies was useful to reveal the potential of fused images for mapping and improve classification accuracy of cerrado. semideciduous and deciduos forests in Minas Gerais. Brazil.

The proposed data fusion and feature extraction method performed well in terms of overall accuracies when compared to results obtained by the original time series of NDVI.

5 REFERENCES

ACERBI-JUNIOR, F.W.; CLEVERS, J.G.P.W.; SCHAEPMAN, M.E. The assessment of multi-sensor image fusion using wavelet transform for mapping the Brazilian savanna. **International Journal of Applied Earth Observation and Geoinformation**, n.8, p.218-288, 2006.

ACERBI-JUNIOR, F.W.; CARVALHO, L.M.T.; WACHOWICZ, M.; CLEVERS, J.G.P.W. Are we using the right quality measures in multi-resolution data fusion? In: EARSEL SYMPOSIUM " NEW STRATEGIES FOR EUROPEAN REMOTE SENSING", 24., 2004, Dubrovnik. **Proceedings**... Dubrovnik, Croatia: Mill, 2004. p.361-368.

AIAZZI, B.; ALPARONE, L.; BARONTI, S.; GARZELLI, A. Context-driven fusion of high spatial and spectral resolution images based on oversampled multiresolution analysis. **IEEE Trans. Geosci. Remote Sens**., v.40, n.10, p.2300-2312, 2002.

BRUCE, L.M.; MARTHUR, A.; BIRD JR., J.D. Denoising and wavelet-based feature extraction of MODIS multi-temporal vegetation signatures. **GIScience & Remote Sensing**, n.43, p.170-180, 2006.

CARVALHO, L.M.T. **Mapping and monitoring forest remnants**: a multiscale analysis of spatio-temporal data. 2001. 138p. Thesis (Doctor in Geoscience) – Wageningen University, Wageningen.

CHAPMAN, L.J.; ORR, T.M. Wavelets and fusion. **Proceedings of the International Congress on Image Processing**, p.248–251, 1995.

CHIBANI, Y.; HOUACINE, A. Multiscale versus multiresolution analysis for multisensor image fusion. **Proceedings of the European Signal Processing Conference**, Island of Rhodes, Greece, p.451–454, 2003.

CONGALTON, R.G.G.; GREEN, K. **Assessing the accuracy of remotely sensed data:** principles and practices. New York: Lewis, 1999. 137p.

HOLSCHNEIDER, M.; KRONLAND-MARTINET, R.; MORLET, J., TCHMITCHIAN, P. A real time algorithm for signal analysis with the help of the wavelet transform. In: COMBES J.M.; GROSSMAN, A.; TCHMITCHIAN, P. (Ed.). **Wavelets:** time frequency methods and phase space**.** New York: Springer-Verlag, 1989. p.286-297..

HUETE, A.R.; LIU, H.Q.; BATCHILY, K.; VAN LEEUWEN, W. A comparison of vegetation indices over a global set of TM images for EOS-MODIS. **Remote Sensing of Environment**, n.59, p.440–451, 1997.

JUSTICE, C.O.; VERMOTE, E.; TOWNSHEND, J.R.G.; DEFRIES, R.; ROY, D.P.; HALL, D.K.; SALOMONSON, V.V.; PRIVETTE, J.L.; RIGGS, G.; STRAHLER, A.; LUCHT, W.; MYNENI, R.B.; KNYAZIKHIN, Y.; RUNNING, S.W.; NEMANI, R.R.; WAN, Z.M.; HUETE, A.R.,;VAN LEEUWEN, W.; WOLFE, R.E.; GIGLIO, L.; MULLER, J.P.; LEWIS, P.; BARNSLEY, M.J. The moderate resolution imaging spectroradiometer (MODIS): land remote sensing for global change research. **IEEE Transactions on Geoscience and Remote Sensing**, n.36, p.228–1249, 1997.

MEENAKSHISUNDARAM, V.; COULOIGNER, I. Image fusion of IKONOS pan and multispectral images for classification of the urban environment. In: EARSEL SYMPOSIUM "NEW STRATEGIES FOR EUROPEAN REMOTE SENSING", 24., 2004, Dubrovnik. **Proceedings...** Dubrovnik, Croatia: Mill, 2004. p.335-345.

NÚÑES, J.; OTAZU, X.; FORS, O.; PRADES, A.; PALA, V.; ARBIOL, R. Multiresolution-based image fusion with additive wavelet decomposition. **IEEE Transactions on Geoscience and Remote Sensing**, n.37, n.3, p.1204-1211, 1999.

POHL, C. **Geometric aspects of multisensory image fusion for topographic map updating in the humid tropics**. International Institute for Aeroespace Survey and Earth Sciences, 1996. v.39, 159p.

QUINLAN, J.R. **Programs for machine learning**. Amsterdam: M. Kaufmann, 1993. 328p.

RANCHIN, T.; AIAZZI, B.; ALPARONE, L.; BARONTI, S.; WALD, L. Image fusion – the ARSIS concept and some successful implementation schemes. **Isprs J. Photogrammetric Remote Sensing**, v.58, n.1-2, p.4-18, 2003.

REED, B.C.; BROWN, J.F.; VANDERZEE, D.; LOVELAND, T.R.; MERCHANT, J.W; OHLEN, D.O. Measuring phenological variability from satellite imagery. **Journal of Vegetation Science**, n.5, p.703–714, 1994.

SADER, S.A.; STONE, T.A.; JOYCE, A.T. Remote sensing of tropical forests: an overview of research and applications using no photographic sensors.

Photogrammetric Engineering and Remote Sensing, v.56, p.1343–1351, 1990.

SHENSA, M.J. The discrete wavelet transform: wedding the a trous and Mallat algorithms. **IEEE Trans. Signal Process**, n.40, p.2464–2482, 1992.

STARCK J.L.; MURTAGH, F.; BIJAOUI, A. **Image Processing and Data Analysis.** Cambridge: University of Cambridge, 1998. 286p.

ZHANG, X.; SOHLBERG, R. A.; TOWNSHEND, J.R.G.; DIMICELI, C.; CARROLL, M.L.; EASTMAN, J.C. Detection of land cover changes using MODIS 250 m data. **Remote Sensing of Environment**, n.83, p.336–350, 2002.

WILSON, T.A.; ROGERS, S.K.; MYERS, L.R. Perceptual-based hyperspectral image fusion using multiresolution analysis. **Opt. Eng**., v.34, n.11, p.3145–3164, 1995.

CHAPTER 05

1 GENERAL CONCLUSION

This work was based on the following hypothesis: The spectral behavior of the land cover classes may be identified when they are analyzed along the annual cycle. including both the dry and the rainy seasons. Thus. long time series combined with feature extractions algorithms and image fusion can be used to improve the separation of spectrally similar objects and produce accurate maps.

To validate this hypothesis the following research questions were done:
(1)Can MODIS vegetation indices depict vegetation dynamics? (**Chapter 02**)
(2)Can feature extractions algorithms improve classification accuracy? (**Chapter 03**)
(3)Can image fusion combined with feature extraction algorithm improve classification accuracy? (**Chapter 04**)

Responding these questions we can concluded that:

(1) The vegetation indices (NDVI and EVI) temporal profiles were efficient to depict the seasonal dynamics of vegetation and the best index for mapping was the NDVI;

(2) The wavelet decomposition improved land cover classification accuracy when the algorithm used in the transformation and the levels were properly chosen;

(3) The data fusion and feature extraction method performed well in terms of overall accuracy as well as in terms of classes compared to results obtained by the original time series of NDVI.

According to all feature vectors used in the classification process we can conclude that:

(1) The best feature vector to classify the cerrado class considering the producer accuracy is the third scale linear spline smothed NDVI time series (99.33%). however considering the user accuracy. the best feature vector is time series of NDVI fused images (100%) or second scale cubic spline smothed NDVI fused images (100%).

(2) The best feature vector to classify the deciduous class considering the producer accuracy is the second scale cubic spline smothed NDVI fused images (99.67%). however considering the user accuracy. the best feature vector is the first scale cubic spline smothed NDVI fused images (100%) or the first scale linear cubic smothed NDVI fused images (100%).

(3) The best feature vector to classify the semideciduous class considering the producer accuracy is the Second scale linear spline smothed NDVI time series (88.5%). however considering the user accuracy. the best feature vector is the first scale linear spline smothed NDVI time series (94.44%).

According to these results is clearly seen that each technique is more appropriate to classify each vegetation type and depends to the accuracy measure that is chosen. Table 1 shows the classes accuracy measures.

Table 1. Accuracy measures.

Feature Vector	Error Matrix		Cerrado		Deciduous		Semideciduous	
	Overral Accuracy	Kappa Coefficent	Producer Accuracy	User Accuracy	Producer Accuracy	User Accuracy	Producer Accuracy	User Accuracy
Time series of NDVI	89.93	0.86	90.17	90.62	89.67	98.90	75.00	78.95
Time series of EVI	87.77	0.82	92.00	89.61	80.00	94.12	85.00	73.91
First scale linear spline smothed NDVI time series	86.32	0.80	91.33	86.67	83.67	96.54	59.50	94.44
Second scale linear spline smothed NDVI time series	90.42	0.87	90.83	93.80	86.33	94.53	88.50	92.19
Third scale linear spline smothed NDVI time series	85.07	0.79	84.5	90.70	83.00	84.40	76.50	81.40
First scale cubic spline smothed NDVI time series	81.60	0.74	84.17	85.45	73.67	96.09	61.50	68.72
Second scale cubic spline smothed NDVI time series	81.04	0.73	82.83	87.19	78.33	95.53	64.50	75.00
Third scale cubic spline smothed NDVI time series	81.18	0.74	76.00	88.37	83.33	73.53	76.50	82.26
Time series of NDVI fused images	94.09	0.91	97.50	100.00	95.67	97.29	82.00	85.42
First scale linear spline smothed NDVI fused images	83.95	0.77	98.17	79.17	94.00	100.00	86.00	86.87
Second scale linear spline smothed NDVI fused images	89.30	0.85	96.67	99.83	98.67	82.91	71.50	81.25
Third scale linear spline smothed NDVI time series	92.50	0.89	99.33	97.07	98.67	83.08	81.00	83.94
First scale linear cubic smothed NDVI fused images	92.48	0.90	96.67	99.49	98.33	100.00	72.50	84.80
Second scale cubic spline smothed NDVI fused images	95.41	0.93	97.67	100.00	99.67	98.03	86.00	87.31
Third scale cubic spline smothed NDVI fused images	90.90	0.87	93.50	93.39	93.67	89.78	81.00	81.82